Backbone Dynamics of the First, Second, and Third Immunoglobulin Modules of the Neural Cell Adhesion Molecule (NCAM)†

Thorsten Thormann,‡ Vladislav Soroka,§ Steen Nielbo,‡ Vladimir Berezin,§ Elisabeth Bock,§ and Flemming M. Poulsen*,‡

Department of Protein Chemistry, Institute of Molecular Biology, University of Copenhagen, Øster Farimagsgade 2A, DK-1353 Copenhagen, Denmark, and the Protein Laboratory, Institute of Molecular Pathology, University of Copenhagen, Blegdamsvej 3C, Building 6.2, DK-2200 Copenhagen, Denmark

Received March 3, 2004; Revised Manuscript Received June 11, 2004

ABSTRACT: The neural cell adhesion molecule (NCAM) is a cell surface multimodular protein, which plays an important role in cell−cell adhesion by homophilic (NCAM−NCAM) and heterophilic (NCAM−non-NCAM molecules) binding. In the present study, the backbone dynamics of the first three immunoglobulin-like (Ig) modules of NCAM have been investigated by NMR spectroscopy. Ig1, Ig2, and Ig3 share low sequence identity but possess the same fold and have very similar three-dimensional structures. ^{15}N longitudinal and transverse relaxation rates and heteronuclear NOEs have been measured and subsequently analyzed by the axial symmetric Lipari−Szabo modelfree formalism to characterize fast (pico- to nanosecond) and slow (micro- to millisecond) motions in the three protein modules. We found that backbone motions of residues located in the β-strand regions are generally restricted, while increased flexibility is observed in turns and loops. In all three modules, residues located in the segments connecting the C- and D-strand plus residues located in the segment connecting the E- and F-strand show significant chemical exchange on the micro- to millisecond time scale. In addition, a number of residues with small chemical exchange contribution seem to form contiguous regions in the β sheets, suggesting that these motions might be correlated. Only few residues in the homophilic binding sites in the NCAM Ig1 and Ig2 modules show increased flexibility, indicating that the Ig1−Ig2-mediated NCAM homophilic binding does not depend on the local backbone mobility of the interacting modules.

The neural cell adhesion molecule (NCAM)[1] belongs to the Ig superfamily (IgSF) of cell-adhesion molecules. It mediates Ca^{2+}-independent cell−cell adhesion by homophilic binding, where NCAM molecules on opposing cell membranes bind each other (*1*). This homophilic NCAM binding plays an important role in many processes such as differentiation, survival, and neuronal plasticity (*2*). Alternative splicing of mRNA generates three major NCAM isoforms, which have identical extracellular parts consisting of five N-terminal Ig-like modules followed by two fibronectin type III (Fn3) repeats. The molecular mechanisms of the NCAM-mediated cell−cell recognition and complex formation have been studied extensively, but it is still controversial which of the extracellular modules are involved and how they interact (*3*−*9*). The three-dimensional structures of the Ig1, Ig2, and Ig3 modules have been determined by NMR spectroscopy and classified as I1 set of Ig modules (*7*, *9*, *10*). The structures of the Ig1−Ig2 double module and the Ig1−Ig2−Ig3 triple module fragments have been determined by X-ray crystallography (*8*, *11*). Both structures indicate that the contacts between Ig1 and Ig2 are very important for the NCAM homophilic binding.

NMR spin relaxation methods are widely used to study protein dynamics in solution, and for many proteins, a relationship between protein flexibility and function has been documented. Flexible parts of a protein backbone are often associated with a ligand-binding site or residues important for the biological function (*12*−*14*). In the present work, the backbone dynamics of recombinant Ig1, Ig2, and Ig3 rat NCAM have been analyzed to determine common dynamic properties of the Ig fold and features that might be related to homophilic cell−cell adhesion in NCAM.

MATERIALS AND METHODS

Uniformly ^{15}N-labeled samples of rat NCAM Ig1, Ig2, and Ig3 were prepared and purified as described previously (*7*, *10*). NMR signal assignment and structural data of Ig1 and Ig2 modules have already been published (*7*), and similar data for Ig3 are in preparation (Soroka et al., unpublished data). These assignments were used in the analysis of the backbone dynamics. Dynamic information was obtained from measurements of the ^{15}N-relaxation time constants (T_1 and T_2) and heteronuclear ^{1}H-^{15}N NOEs using sensitivity-enhanced proton-detected pulse schemes (*14*) on 0.7, 1, and 3.5 mM samples of uniformly ^{15}N-labeled Ig1, Ig2, and Ig3,

† This work was supported by the John and Birthe Meyer Foundation, the Danish Medical Research Council, and the Lundbeck Foundation.

* To whom correspondence should be addressed. Phone: +45 353 22077. Fax: +45 353 22075. E-mail: fmp@apk.molbio.ku.dk.

‡ Institute of Molecular Biology.

§ Institute of Molecular Pathology.

[1] Abbreviations: NCAM, neural cell adhesion molecule; Ig, immunoglobulin-like; Ig1, first module of NCAM; Ig2, second module of NCAM; Ig3, third module of NCAM; NOE, nuclear Overhauser effect; NMR, nuclear magnetic resonance.

10.1021/bi0495679 CCC: $27.50
Published on Web 07/21/2004

respectively, For the Ig3, the ^{15}N-relaxation time measurements (T_1 and T_2) were repeated on a sample of 0.7 mM. The samples were prepared in 5 mM phosphate buffer at pH 7.4 and 150 mM NaCl in 90% H_2O/10% D_2O. All NMR data were acquired at 25 °C on a Varian Unity 750 MHz spectrometer equipped with a triple resonance probe and pulsed-field gradients. Spectra for determination of T_1 and T_2 of Ig1 and Ig2 were recorded using spectral widths of 3200 × 12 000 Hz and acquisition sizes of 128 × 1890 complex points in the $t_1 \times t_2$ dimensions with 16 transients per t_1 experiment and a recycle delay of 1.5 s. For Ig3, the acquisition sizes were increased to 256 × 1890 complex points, while only 8 transients were necessary because of the higher protein concentration. T_1 experiments were recorded with 10 delays of 10, 50, 150, 200, 300, 330, 450, 600, 800, and 1200 ms, and T_2 experiments were recorded with 10 delays of 10, 30, 50, 70, 90, 110, 150, 190, 210, and 250 ms. ^{1}H-^{15}N NOE values were determined from two spectra recorded with and without proton saturation. Spectral widths and acquisition sizes were the same as those for determination of T_1 and T_2, but the number of transients were increased to 32 for each t_1 increment. A recycle delay of 7 s was employed for spectra in the absence of presaturation, whereas a 3 s recycle delay followed by 4 s proton saturation was used in the NOE spectra. All NMR data were processed using NMRPipe software (*15*). The spectra were weighted with a phase-shifted sine bell in t_1 and t_2 and zero-filled to double size in each dimension prior to Fourier transformation. Peak heights were measured using Pronto (*16*). ^{15}N-relaxation times (T_1 and T_2) were determined from a nonlinear least-squares fit of an exponential curve to the measured peak heights. NOE values were determined as the I_{sat}/I_{unsat} ratio, where I_{sat} and I_{unsat} are peak heights in spectra with and without proton saturation. Uncertainties of the NOE values were estimated from the baseline noise (*14*).

RESULTS

The 2D NH-correlated NMR spectra of Ig1, Ig2, and Ig3 are well-resolved and have a high S/N ratio even at the relative high pH of 7.4. T_1 and T_2 were reliably determined for 90 of 96 amide groups in Ig1, 79 of 89 in Ig2, and 88 of 102 in Ig3. For a few residues, the NOEs exceed unity by up to 10%. This indicates errors in the estimated peak heights in the NOE or NONOE spectra. Such effects could arise from insufficient proton saturation in the NOE experiment or the presence of residual saturation in the NONOE experiment. Special care was taken to avoid either of these two cases, and because no systematic deviation seems to be present in the data, this is unlikely to be the explanation. It is more likely, that artifacts in the NOEs are introduced at solvent-exposed positions with fast exchange between amide and solvent protons, which is especially pronounced at the elevated pH of 7.4. Relaxation parameters for the residues in question were eliminated from further analysis. For Ig3 the R_1 and R_2 were measured at two concentrations 0.7 and 3.5 mM. The comparison showed that the average R_1 was 1.4 ± 0.1 and 1.3 ± 0.1 s^{-1} at 0.7 and 3.5 mM, respectively, and correspondingly for R_2, 11.2 ± 0.8 and 10.8 ± 0.8 s^{-1}. The concentration dependence corresponds to a marginal difference in the derived correlation time of 6.9 ± 0.2 and 6.7 ± 0.3 ns. The correlation time for Ig1 and Ig2 were 5.4 ± 0.2 and 5.6 ± 0.2 ns, respectively.

The relaxation parameters of Ig1, Ig2, and Ig3 were analyzed by Lipari−Szabo modelfree formalism (*17*). In this model, the internal motions are described in terms of an overall rotational diffusion tensor for the molecule, a generalized order parameter, and an internal correlation time. The relaxation rates are dependent on the orientation of the relaxation mechanisms, relative to the rotational diffusion tensor of the molecule (*18*), and even a small degree of anisotropy can introduce errors in the dynamical parameters (*19*, *20*). To evaluate the degree of anisotropy for Ig1, Ig2, and Ig3, hydrodynamic calculations of the rotational diffusion tensor were performed with HYDRONMR version 5.0a (*21*). In this way, the three components (D_{xx}, D_{yy}, and D_{zz}) of the rotational diffusion tensor were predicted to 1.89×10^7, 1.85×10^7, and 3.18×10^7 s^{-1} for Ig1; 2.06×10^7, 2.02×10^7, and 3.18×10^7 s^{-1} for Ig2; and 1.37×10^7, 1.34×10^7, and 2.88×10^7 s^{-1} for Ig3. The anisotropy is given by $A = (D_{xx} + D_{yy})/2D_{zz}$. Using this relation, the anisotropy of the three Ig modules in solution can be estimated to 1.7, 1.7, and 2.1 for Ig1, Ig2, and Ig3, respectively, indicating anisotropic tumbling as the values deviate from unity. This calculation indicates that the hydrodynamic properties of Ig1 and Ig2 are very similar, while the tumbling of Ig3 might be slightly more anisotropic. On the basis of this calculation that clearly indicates anisotropic tumbling of all three modules, the axial symmetric modelfree spectral density function (*18*) was chosen to derive the dynamical parameters of the three NCAM modules. Optimization of the rotational diffusion and the modelfree parameters against the experimental data was performed using TENSOR version 2.0 (*22*). In the Lipari−Szabo modelfree treatment, five different models with up to three parameters describing the internal motions were employed. In model 1, only the order parameter S^2 is optimized. In model 2, S^2 and the internal correlation time τ_i are optimized. Model 3 is identical to model 1 but with addition of the exchange contribution R_{ex} to R_2. Model 4 is the same as model 2 but includes R_{ex}. In model 5, S^2, the fast motion order parameter S_f^2, and τ_i are optimized. Model selection is based on extensive *F*-statistical testing and implemented in TENSOR version 2.0 (*22*). The experimental relaxation parameters R_1, R_2, and ^{1}H-^{15}N NOEs plus the modelfree variables S^2 and R_{ex} are plotted against the residue number in Figures 1−3. S^2 reflects fast motions in the nano- to picosecond range (10^{-9}−10^{-12} s), whereas the R_{ex} is related to slower motions from the interchange between different molecular conformations on the milli- to microsecond (10^{-3}−10^{-6} s) time scale. R_{ex} is a function of the chemical-shift differences, the equilibrium populations of different conformational states, and the exchange rates between these states. Slow exchange between different species results in overestimation of R_2 from the relaxation dispersion curves, where $R_2^{obs} = R_2^0 + R_{ex}$, which clearly can be seen from the experimental data (Figures 1−3), where R_{ex} systematically is modeled for residues with increased R_2 values. Because the exchange rates between the different conformations are not determined in these experiments, R_{ex} is interpreted only qualitatively.

The average order parameters S^2 are within the range of their standard deviations and very similar for the Ig1, Ig2, and Ig3 modules: 0.87 ± 0.11, 0.88 ± 0.06, and 0.81 ± 0.08, respectively. Only a few residues in Ig1 and Ig3 were

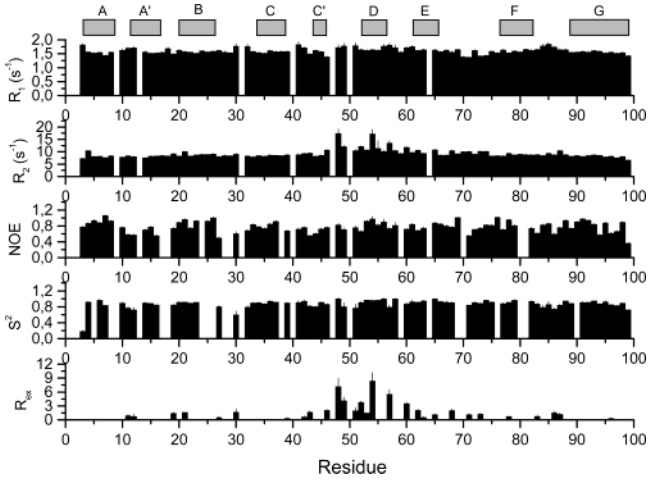

FIGURE 1: Relaxation and modelfree parameters determined for NCAM Ig1. From the top: the longitudinal relaxation rate constant R_1, the transverse relaxation rate constant R_2, the heteronuclear ^{1}H-^{15}N NOE, the order parameter S^2, and the chemical exchange contribution R_{ex}. All parameters are shown as a function of the residue number. Positions of the β strands are marked in the top of each diagram.

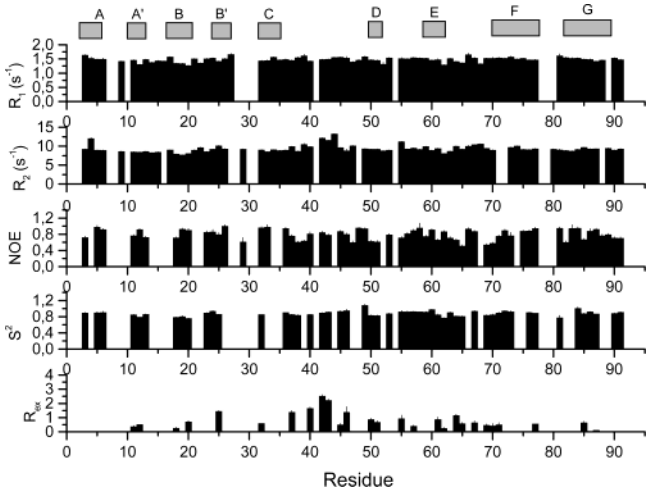

FIGURE 2: Relaxation and modelfree parameters determined for NCAM Ig2. From the top: the longitudinal relaxation rate constant R_1, the transverse relaxation rate constant R_2, the heteronuclear ^{1}H-^{15}N NOE, the order parameter S^2, and the chemical exchange contribution R_{ex}. All parameters are shown as a function of the residue number. Positions of the β strands are marked in the top of each diagram.

found to have order parameters smaller than 0.7, which is typically the lower limit for residues in regular secondary structure (*20*). These observations indicate that all three modules have quite rigid backbone structures. From the upper panels in Figure 1, it can be seen that the S^2 value deviates along the backbone in all three modules. Lower values are typically found in or near turns and loops but not restricted to these regions. A number of residues exhibit increased R_{ex} values, indicating higher mobility on the micro- to millisecond time scale. Most of these residues are found in the CD loop, the D strand, and the EF turn in all three modules (Figures 5 and 6).

In the HSQC spectrum of Ig3, it appears that several signals are present in dublo. The origin of these doublet signals from one single atom has been controlled in a ^{15}N-TOCSY−HSQC experiment, showing that both peaks originate from the same NH group. Amino acid sequencing and MALDI−TOF mass spectroscopy have shown only one polypeptide chain present in the sample. Moreover, it was not possible to eliminate one of the sets by further purification, indicating that the protein is present in two forms in solution. Attempts to measure exchange cross peaks between the two signals using an exchange experiments (*19*) failed, suggesting that the exchange between the two forms is very slow. Because the ^{15}N-relaxation rate constants are nearly identical for both peaks (Figure 4) they have been considered as one in the analysis of the backbone dynamics.

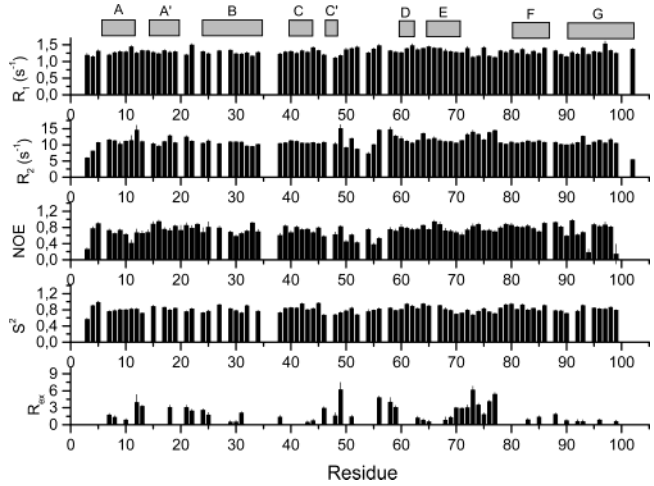

FIGURE 3: Relaxation and modelfree parameters determined for NCAM Ig3. From the top: the longitudinal relaxation rate constant R_1, the transverse relaxation rate constant R_2, the heteronuclear ^{1}H-^{15}N NOE, the order parameter S^2, and the chemical exchange contribution R_{ex}. All parameters are shown as a function of the residue number. Positions of the β strands are marked in the top of each diagram.

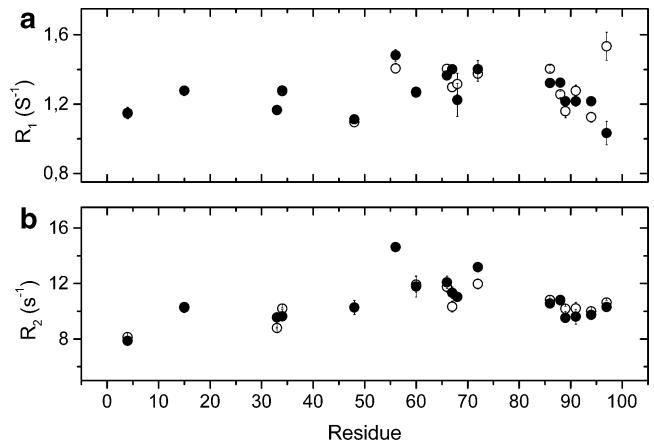

FIGURE 4: Relaxation rate constants for peaks that appear twice in the ^{15}N-HSQC spectrum of Ig3. The two different values of the relaxation parameter belonging to the same residue are shown as ○ and ●, respectively. (a) R_1 values and (b) R_2 values.

DISCUSSION

General Trends in Backbone Dynamics of the Three Ig Modules of NCAM. The overall dynamical landscapes of the three Ig modules have much in common. Apart from a few exceptions, the residues occupying the centers of the β strands have more restricted motions on the fast time scale than residues located in loops and turns. Because the core regions have more inter-residue contacts, it is not surprising

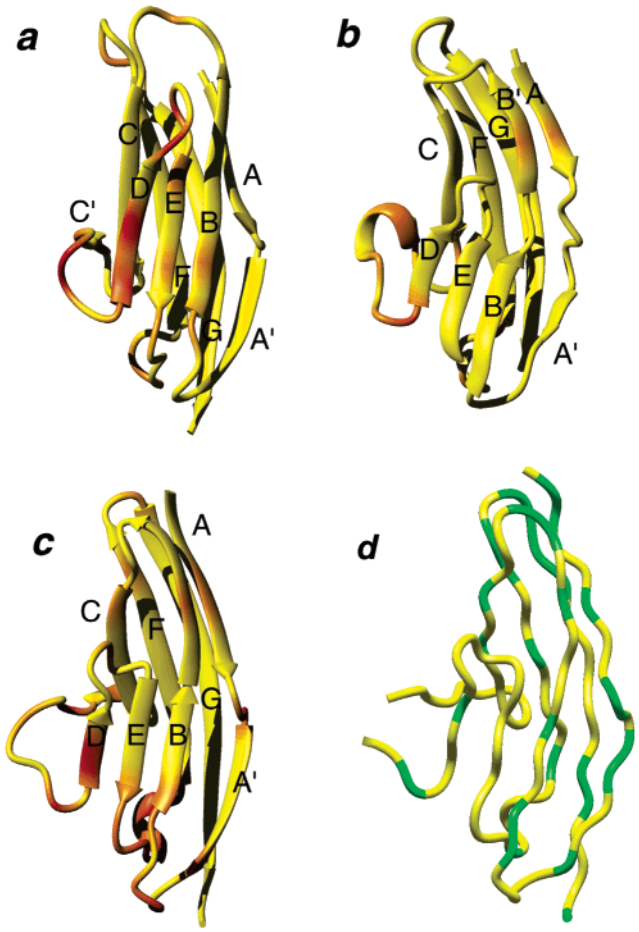

FIGURE 5: Mapping of residues showing increased flexibility on the micro- to millisecond time scale in Ig1 (a), Ig2 (b), and Ig3 (c). Residues are colored according to the R_{ex} value: $R_{ex} < 1$ are in yellow, $1 < R_{ex} < 2$ are in orange, $2 < R_{ex} < 3$ are in dark orange, $3 < R_{ex} < 5$ are in orange red, and $5 < R_{ex}$ are in red. β strands are labeled from A to G. The depicted structures of Ig1 and Ig2 are NMR solution structures (*7*, *10*), whereas the structure of Ig3 has been determined by X-ray crystallography (*11*). (d) Residues in the Ig3 module showing a set of two resonances.

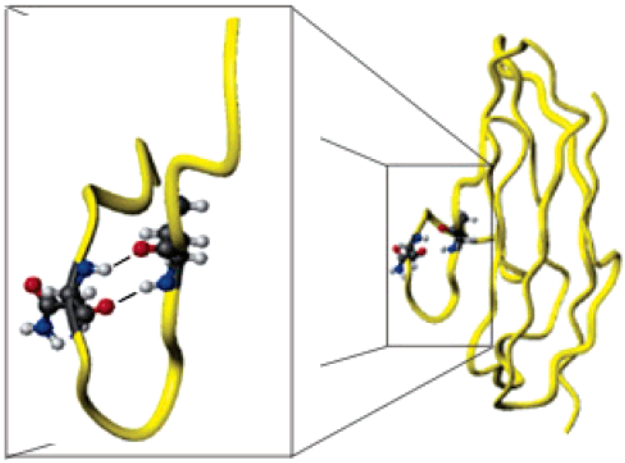

FIGURE 6: Asn48 and Val54 in Ig1. Breakage and reformation of hydrogen bonds between Asn48 and Val54 may explain the high exchange contribution observed for these two residues.

that they are constrained more strongly. Interestingly, the indications of conformational fluctuations on the micro- to millisecond time scale are found for several residues. The CD loop and the EF turn connecting the two β sheets both have significantly increased flexibility on the micro- to millisecond time scale. Exchange in the CD loop is most pronounced in Ig1 and Ig2, while exchange in the EF turn is highest in Ig3, but increased flexibility is found in both regions in all three modules. In addition, several other residues have exchange terms but with a much lower amplitude, and these residues seem to be forming contiguous regions in all three modules. These regions span across two or three β strands: Phe21, Ser53, and Thr65 in Ig1; Phe4 and Val25 in Ig2; and Ser24, His58, and Arg70 in Ig3. Similar patterns of residues showing conformational fluctuations on the microsecond time scale have been reported for the third Fn3 module of tenacin-C, where it is suggested to indicate collective motions such as breathing or twisting of the β sheets (*25*). This protein module also forms a β sandwich and has a topology similar to C2-set Ig modules, even though Fn3 and Ig modules do not share sequence homology (*26*). Inspection of the Ig1, Ig2, and Ig3 structures does only in some cases show a correlation between local structural elements, such as interstrand hydrogen bonds and increased motional amplitude. A clear example is found in Ig1, where motions in the CD loop seem to be associated with dynamics in the residues of the D strand. Although there is no direct evidence for this, these results may be explained by dynamics originating from the opening and closing of the two hydrogen bonds between the amide and carboxyl groups of Asn48 (located in the CD loop) and Val54 (located in the D strand), giving rise to the mobility reflected in the relaxation data (Figure 6). Other mechanisms are likely for the movements in the CD loop of Ig2 and Ig3 because no similar hydrogen bonds are present. Because the Ig1, Ig2, and Ig3 modules all belong to the I1 set of the Ig superfamily, it is likely that the observed motions of the CD loop and EF turn reflect common dynamic features of this fold.

Functional Aspects of the Observed Backbone Dynamics. The molecular mechanisms of the homophilic interactions and the structure of the homophilic binding complex have been extensively debated because of the disagreement in results obtained from cell-based experiments and structural X-ray and NMR data. Cell aggregation experiments performed on mouse L cells expressing chicken NCAM with deletions of different Ig modules indicated an involvement of the Ig3 module (*27*). Microspheres coated with individual recombinant Ig modules of chicken NCAM demonstrated binding between the Ig1−Ig5 and Ig2−Ig4 modules, whereas microspheres coated with Ig3 exhibited strong self-aggregation (*28*). These findings were not supported by solution studies, where no dimerization of Ig3 was found, whereas interaction between Ig1 and Ig2 was clearly observed (*7*, *9*, *29*, *30*). The crystal structure of Ig1−Ig2 homophilic dimer and the crystal structure of the Ig1−Ig2−Ig3 NCAM fragment further support a model in which Ig1 and Ig2 are directly involved in the NCAM homophilic binding (*8*, *11*). The presence of double peaks in the HSQC spectrum could indicate two different species, with one being the monomer and the other the dimer. Because no exchange between the two species can be observed and both components of the double peaks have the same relaxation rate constants, a monomer−dimer model does not seem to be the explanation. Significant differences in the relaxation parameters would be expected between a monomer and a dimer because of

differences in size and shape. When all three modules are compared, it is observed that the averages of R_1 are 1.6 ± 0.2 s^{-1}, 1.5 ± 0.1 s^{-1}, and 1.3 ± 0.1 s^{-1} and the averages of R_2 are 8.9 ± 1.9 s^{-1}, 9.4 ± 0.4 s^{-1}, and 10.9 ± 0.8 s^{-1} for Ig1, Ig2, and Ig3, respectively. These average values are based on only 80% of the residues because the residues with lowest and highest R_1 and R_2 values were eliminated from the calculation. Regarding Ig3, $\langle R_1 \rangle$ are slightly lower than for Ig1 and Ig2 and $\langle R_2 \rangle$ are slightly higher. The concentration dependence of the $\langle R_1 \rangle$ and $\langle R_2 \rangle$ for Ig3 was seen to be very small and most likely reflecting increased viscosity in the more concentrated sample. Bearing in mind the very strong Ig3−Ig3 interactions observed in aggregation experiments (*28*), the relaxation properties observed using NMR are not very pronounced even in a relatively concentrated sample at 3.5 mM. It is more likely that differences in the relaxation parameters between Ig1/Ig2 and Ig3 are an effect of slower molecule tumbling in the sample of Ig3, which has a higher viscosity because of the higher protein concentration. Therefore, our results show that there is no strong Ig3−Ig3 interaction in solution in agreement with previous solution studies of Ig3 from chicken (*9*, *30*).

In the earlier studies, the homophilic binding sites in Ig1 and Ig2 have been located in a series of NMR titration experiments (*7*, *9*). We find that residues with high exchange contribution in the CD loop are located at the rim of the binding interface in both Ig1 and Ig2, and local structural fluctuations at these positions do not seem to be directly involved in the binding. Phe21 and Thr65 in Ig1 are in the binding interface, but the motional amplitudes of these two residues are small. It does not seem likely that movements in these two residues alone facilitate the complex formation by an induced fit mechanism. Large surface areas are buried in the binding complex (*8*, *11*). Therefore, it is likely that low amplitude collective fluctuations in the backbone play a role by inducing structural adaptability in the binding interface. Similar observations have been observed for the bacterial response regulator protein Spo0F, where regions having motion on the millisecond time scale correlate with residues and surfaces that are known to be critical for protein−protein interactions (*31*), and in the enzyme cyclophilin, where submillisecond dynamics has been observed for residues near the catalytic site (*32*). The observed higher mobility in the EF turn and the CD loop together with the lower amplitude pervasive motions in the β sheets might reflect such fluctuations.

CONCLUSION

We found that the backbone dynamics of NCAM Ig1, Ig2, and Ig3 modules are very similar. Because the three modules do not share high sequence identity but have the same fold, we believe that the increased backbone flexibility of linkers between the two β sheets is a structural feature of the Ig fold, whereas the smaller pervasive exchange contributions are sequence-dependent. No direct correlation between flexible segments of the Ig1 and Ig2 modules and their homophilic binding sites were found. It is likely that small fluctuations, as found for a number of sites in the Ig1, Ig2, and Ig3 modules, rather than specific local mobility, are important for the functions of the Ig modules.

ACKNOWLEDGMENT

The authors thank Associate Professor Søren Kristensen for helpful discussions.

REFERENCES

1. Rutishauser, U., Hoffman, S., and Edelman, G. M. (1982) Binding properties of a cell adhesion molecule from neural tissue, *Proc. Natl. Acad. Sci. U.S.A. 79*, 685−689.
2. Ditlevsen, D. K., Kohler, L. B., Pedersen, M. V., Risell, M., Kolkova, K., Meyer, M., Berezin, V., and Bock, E. (2003) The role of phosphatidylinositol 3-kinase in neural cell adhesion molecule-mediated neuronal differentiation and survival, *J. Neurochem. 84*, 546−556.
3. Rao, Y., Wu, X. F., Yip, P., Gariepy, J., and Siu, C. H. (1993) Structural characterization of a homophilic binding site in the neural cell adhesion molecule, *J. Biol. Chem. 268*, 20630−20638.
4. Rao, Y., Zhao, X., and Siu, C. H. (1994) Mechanisms of homophilic binding mediated by the neural cell adhesion molecule NCAM, *J. Biol. Chem. 269*, 27540−27548.
5. Sandig, M., Rao, Y., and Siu, C. H. (1994) The homophilic binding site of the neural cell adhesion molecule NCAM is directly involved in promoting neurite outgrowth from cultured neural retinal cells, *J. Biol. Chem. 269*, 14841−14848.
6. Sandig, M., Rao, Y., Kalnins, V. I., and Siu, C. H. (1996) Integrity of the homophilic binding site is required for the preferential localization of NCAM in intercellular contacts, *Biochem. Cell Biol. 74*, 373−381.
7. Jensen, P. H., Soroka, V., Thomsen, N. K., Ralets, I., Berezin, V., Bock, E., and Poulsen, F. M. (1999) Structure and interactions of NCAM modules 1 and 2—Basic elements in neural cell adhesion, *Nat. Struct. Biol. 6*, 486-493.
8. Kasper, C., Rasmussen, H., Kastrup, J. S., Ikemizu, S., Jones, E. Y., Berezin, V., Bock, E., and Larsen, I. K. (2000) Structural basis of cell−cell adhesion by NCAM, *Nat. Struct. Biol. 7*, 389−393.
9. Atkins, A. R., Chung, J., Deechongkit, S., Little, E. B., Edelman, G. M., Wright, P. E., Cunningham, B. A., and Dyson, H. J. (2001) Solution structure of the third immunoglobulin domain of the neural cell adhesion molecule N-CAM: Can solution studies define the mechanism of homophilic binding? *J. Mol. Biol. 311*, 161−172.
10. Thomsen, N. K., Soroka, V., Jensen, P. H., Berezin, V., Kiselyov, V. V., Bock, E., and Poulsen, F. M. (1996) The three-dimensional structure of the first domain of neural cell adhesion molecule, *Nat. Struct. Biol. 3*, 581−585.
11. Soroka, V., Kolkova, K., Kastrup, J. S., Diederichs, K., Breed, J., Kiselyov, V., Poulsen, F. M., Larsen, I. K., Welte, W., Berezin, V., Bock, E., and Kasper, C. (2003) Structure and interactions of NCAM Ig1−2−3 suggest a novel zipper mechanism for homophilic adhesion, *Structure 11*, 1291−1301
12. Ishima, R. and Torchia, D. A. (2000) Protein backbone dynamics revealed by quasi spectral density function analysis of amide N-15 nuclei, *Nat. Struct. Biol. 7*, 740−743.
13. Wand, A. J. (2001) Dynamic activation of protein function: A view emerging from NMR spectroscopy, *Nat. Struct. Biol. 8*, 926−931.
14. Farrow, N. A., Muhandiram, R., Singer, A. U., Pascal, S. M., Kay, C. M., Gish, G., Shoelson, S. E., Pawson, T., Forman-Kay, J. D., and Kay, L. E. (1994) Backbone dynamics of a free and phosphopeptide-complexed Src homology 2 domain studied by ^{15}N NMR relaxation, *Biochemistry 33*, 5984−6003.
15. Delaglio, F., Grzesiek, S., Vuister, G. W., Zhu, G., Pfeifer, J., and Bax, A. (1995) NMRPipe: A multidimensional spectral processing system based on UNIX pipes, *J. Biomol. NMR 6*, 277−293.
16. Kjaer, M., Andersen, M. K., and Poulsen, F. M. (1994) Automated and semiautomated analysis of homo- and heteronuclear multidimensional nuclear magnetic resonance spectra of proteins; the program Pronto, *Methods Enzymol. 239*, 288−307.
17. Lipari and Szabo (1982) Model-free approach to the interpretation of nuclear magnetic resonance relaxation in macromolecules. 1. Theory and range of validity, *J. Am. Chem. Soc. 104*, 4546−4559.
18. Schurr, J. M., Babcock, H. P. and Fujimoto, B. S. (1994) A test of the model-free formulas. Effects of anisotropic rotational diffusion and dimerization, *J. Magn. Reson., Ser. B 105*, 211−224.

19. Luginbuhl, P., Pervushin, K., Iwai, H., and Wüthrich, K. (1997) Anisotropic molecular rotational diffusion in ^{15}N spin relaxation studies of protein mobility, *Biochemistry 36*, 7305−7312.
20. Osborne, M. J., and Wright, P. E. (2001) Anisotropic rotational diffusion in model-free analysis for a ternary DHFR complex, *J. Biomol. NMR 19*, 209−230.
21. Gacia de la Torre, J., Huertas, M. L., and Carrasco, B. (2000) HYDRONMR: Prediction of NMR relaxation of globular proteins from atomic-level structures and hydrodynamic calculations, *J. Magn. Reson. 147*, 138−146.
22. Dosset, P., Hus, J. C., Blackledge, M., and Marion, D. (2000) Efficient analysis of macromolecular rotational diffusion from heteronuclear relaxation data, *J. Biomol. NMR 16*, 23−28.
23. Farrow, N. A., Zhang, W., Forman-Kay, J. D., and Kay, L. E. (1994) A heteronuclear correlation experiment for simultaneous determination of ^{15}N longitudinal decay and chemical exchange rates of systems in slow equilibrium, *J. Biomol. NMR 4*, 727−734.
24. Engelke, J., and Rüterjans, H. (1999) in *Biological Magnetic Resonance* (Krishna, N. R., and Berliner, L. J., Eds.) pp 357−418, Kluwer Academic, New York.
25. Akke, M., Liu, J., Cavanagh, J., Erickson, H. P., and Palmer, A. G., III (1998) Pervasive conformational fluctuations on microsecond time scales in a fibronectin type III domain, *Nat. Struct. Biol. 5*, 55−59.
26. Vaughn, D. E., and Bjorkman, P. J. (1996) The (Greek) key to structures of neural adhesion molecules, *Neuron 16*, 261−273.
27. Rao, Y., Wu, X. F., Gariepy, J., Rutishauser, U., and Siu, C. H. (1992) Identification of a peptide sequence involved in homophilic binding in the neural cell adhesion molecule NCAM, *J. Cell Biol. 118*, 937−949.
28. Ranheim, T. S., Edelman, G. M., and Cunningham, B. A. (1996) Homophilic adhesion mediated by the neural cell adhesion molecule involves multiple immumoglobulin domains, *Proc. Natl. Acad. Sci. U.S.A. 93*, 4071−4075.
29. Kiselyov, V. V., Berezin, V., Maar, T. E., Soroka, V., Edvardsen, K., Schousboe, A., and Bock, E. (1997) The first Ig-like NCAM domain is involved in both double reciprocal interaction with the second Ig-like NCAM domain and in heparin binding, *J. Biol. Chem. 272*, 10125−10134.
30. Atkins, A. R., Osborne, M. J., Lashuel, H. A., Edelman, G. M., Wright, P. E., Cunningham, B. A., and Dyson, H. J. (1999) Association between the first two immunoglobulin-like domains of the neural cell adhesion molecule N-CAM, *FEBS Lett. 451*, 162−168.
31. Feher, V. A, and Cavanagh, J. (1999) Millisecond-timescale motions contribute to the function of the bacterial response regulator protein Spo0F, *Nature 400*, 289−293.
32. Eisenmesser, E. Z., Bosco, D. A., Akke**,** M, and Kern, D. (2002) Enzyme dynamics during catalysis, *Science 295*, 1520−1523.

BI0495679